

Communication-Aware Dissipative Control for Networks of Heterogeneous Nonlinear Agents

Ingyu Jang * Leila J. Bridgeman *

* Department of Mechanical Engineering and Material Science, Duke University, Durham, NC 27708 USA (e-mail: ij40@duke.edu; ljb48@duke.edu).

Abstract: Communication-aware control is essential to reduce costs and complexity in large-scale networks. However, it is challenging to simultaneously determine a sparse communication topology and achieve high performance and robustness. This work achieves all three objectives through dissipativity-based, sparsity-promoting controller synthesis. The approach identifies an optimal sparse structure using either weighted ℓ_1 penalties or alternating direction methods of multipliers (ADMM) with a cardinality term, and iteratively solves a convexified version of the NP hard structured optimal control problem. The proposed methods are demonstrated on heterogeneous networks with uncertain and unstable agents.

Keywords: Communication-Aware Control, Robust Control, Networked System Control, Heterogeneous Network, Nonlinear System Control

1 Introduction

Networked control systems arise in many modern applications, such as smart grids, power plants networks, or swarm robotics. Even though classical, fully-connected controllers can stabilize such networks with reasonable robustness, they impose substantial communication demands and often lead to impractical communication infrastructures. On the other hand, fully decentralized controllers, which require no communication between agents, eliminate communication costs entirely but typically yield significantly degraded performance. Consequently, there is a strong need for controller architectures that balance performance and communication efficiency by reducing interconnections among agents while maintaining desirable closed-loop behavior [Jovanović and Dhingra, 2016]. Various controller synthesis methods have been proposed to reduce the communication costs in networked control systems, but designing sparse controllers which are robust and applicable to general heterogeneous nonlinear agents remains a challenging problem. This paper addresses the synthesis of robust, communication-aware, controllers for networks of heterogeneous nonlinear agents by promoting controller sparsity and assuring network-wide stability through the Network Dissipativity Theorem (NDT).

Energy-related analysis is widely accepted in the study of stability for physical and engineering systems. Dissipativity [Willems, 1972; Hill and Moylan, 2003] provides an abstract, energy-based characterization of general nonlinear systems by treating them as input-output mappings, ignoring internal states. A key advantage of this abstraction is its design compositionality [Zakeri and Antsaklis, 2022], meaning that the interconnections of dissipative systems

are themselves dissipative and stable with minimum conditions. The NDT in [Moylan and Hill, 2003; Vidyasagar, 1981] exploits this to assess network-level stability using only the open-loop properties of individual agents. While the theorem has been successfully applied to the synthesis of decentralized controllers for large-scale networks [LoCicero and Bridgeman, 2025], additional mechanisms are required when communication among controllers is necessary to improve the performance of the controller.

A straightforward approach to reducing controller interconnections is to impose an ℓ_0 norm (cardinality) constraint on the optimal control framework. However, optimization problems involving cardinality constraints are NP-hard [Natarajan, 1995], making them intractable for large-scale networked systems. To address this challenge, various sparsity-promoting methods have been developed, including ℓ_1 -norm relaxations [Fardad et al., 2011; Babazadeh and Nobakhti, 2016], gradient-based algorithms [Lian et al., 2017, 2018], and alternating-projection approaches [Lin et al., 2013; Negi and Chakrabortty, 2020]. These methods typically include three stages: initializing a feasible controller, identifying a desirable sparse structure, and improving closed-loop performance by solving the resulting fixed-structure control problem.

This work integrates the NDT and an linear quadratic (LQ) performance objective with sparsity-promoting strategies (weighted ℓ_1 norm and ADMM with a cardinality penalty). Although existing sparsity-promoting methods mitigate the intractability of cardinality constraints, combining them with NDT still results in an NP hard problem due to the presence of high-order matrix inequalities. To resolve this challenge, we employ iterative convex overbounding (ICO) [Warner and Scruggs, 2017], in which the high-order matrix inequalities are overbounded

* This work is supported by ONR Grant No. N00014-23-1-2043.

using the techniques in [Sebe, 2018; Ren et al., 2021], and the resulting convex optimization problems are iteratively solved. This approach yields a sparsely interconnected controller that is robust and applicable to networks of nonlinear and heterogeneous agents.

2 Preliminaries

2.1 Notation

The sets of real, natural numbers, and natural numbers up to n are denoted by \mathbb{R} , \mathbb{N} , \mathbb{N}_n , respectively. The set of real $n \times m$ matrices is $\mathbb{R}^{n \times m}$, and the $(i, j)^{\text{th}}$ block or element of a matrix \mathbf{A} is denoted \mathbf{A}_{ij} . If $\mathbf{A}_{ij} \in \mathbb{R}^{n_i \times m_i}$ and $\mathbf{A} \in \mathbb{R}^{\sum_{i=1}^N n_i \times \sum_{j=1}^M m_j}$, then \mathbf{A}_{ij} is said to be a “block” of \mathbf{A} , and \mathbf{A} is said to be in $\mathbb{R}^{N \times M}$ block-wise. The set of $n \times n$ symmetric matrices is \mathbb{S}^n . The notation $\mathbf{A} \prec 0$ indicates that \mathbf{A} is negative-definite. For brevity, $\text{He}(\mathbf{A}) = \mathbf{A} + \mathbf{A}^T$ and asterisks, $*$, denote duplicate blocks in symmetric matrices. The set of square integrable functions is \mathcal{L}_2 . The Frobenius norm, \mathcal{L}_1 norm, and \mathcal{L}_2 norm are denoted by $\|\cdot\|_F$, $\|\cdot\|_1$ and $\|\cdot\|_2$, respectively. The truncation of a function $\mathbf{y}(t)$ at T is denoted by $\mathbf{y}_T(t)$, where $\mathbf{y}_T(t) = \mathbf{y}(t)$ if $t \leq T$, and $\mathbf{y}_T(t) = 0$ otherwise. If $\|\mathbf{y}_T\|_2^2 = \langle \mathbf{y}_T, \mathbf{y}_T \rangle = \int_0^\infty \mathbf{y}_T^T(t) \mathbf{y}_T(t) dt < \infty$ for all $T \geq 0$, then $\mathbf{y} \in \mathcal{L}_{2e}$, where \mathcal{L}_{2e} is the extended \mathcal{L}_2 space.

2.2 QSR-Dissipativity of Large-Scale Systems

This section reviews the *QSR*-dissipativity and its application to for stability analysis of networks.

Definition 1. (*QSR*-Dissipativity, [Vidyasagar, 1981]). Let $\mathbf{Q} \in \mathbb{S}^l$, $\mathbf{R} \in \mathbb{S}^m$, and $\mathbf{S} \in \mathbb{R}^{l \times m}$. The operator $\mathcal{G} : \mathcal{L}_{2e}^m \mapsto \mathcal{L}_{2e}^l$ is *QSR*-dissipative if there exists $\beta \in \mathbb{R}$ such that for all $\mathbf{u} \in \mathcal{L}_{2e}^m$ and T .

$$\int_0^T \begin{bmatrix} \mathcal{G}(\mathbf{u}(t)) \\ \mathbf{u}(t) \end{bmatrix}^T \begin{bmatrix} \mathbf{Q} & \mathbf{S} \\ * & \mathbf{R} \end{bmatrix} \begin{bmatrix} \mathcal{G}(\mathbf{u}(t)) \\ \mathbf{u}(t) \end{bmatrix} dt \geq 0 \quad (1)$$

We identify *QSR*-dissipativity of linear time-invariant (LTI) systems as follows.

Lemma 1. (Dissipativity Lemma, [Gupta, 1996]). An LTI system with minimal state-space realization $(\mathbf{A}, \mathbf{B}, \mathbf{C}, \mathbf{D})$ is *QSR*-dissipative if there exist a matrix $\mathbf{P} \succ 0$ and matrices \mathbf{Q} , \mathbf{S} , and \mathbf{R} such that

$$\begin{bmatrix} \text{He}(\mathbf{P}\mathbf{A}) - \mathbf{C}^T \mathbf{Q} \mathbf{C} & \mathbf{P} \mathbf{B} - \mathbf{C}^T \mathbf{S} - \mathbf{C}^T \mathbf{Q} \mathbf{D} \\ \mathbf{B}^T \mathbf{P} - \mathbf{S}^T \mathbf{C} - \mathbf{D}^T \mathbf{Q} \mathbf{C} & -\mathbf{R} - \text{He}(\mathbf{S}^T \mathbf{D}) - \mathbf{D}^T \mathbf{Q} \mathbf{D} \end{bmatrix} \preceq 0 \quad (2)$$

Dissipativity is closely related to the input-output (IO)-stability of the system, defined below.

Definition 2. (IO or \mathcal{L}_2 -stability, [Lozano et al., 2013]). An operator $\mathcal{G} : \mathcal{X}_e^m \mapsto \mathcal{X}_e^l$ is IO-stable, if for any $\mathbf{u} \in \mathcal{X}^m$ and all \mathbf{x}_0 where \mathcal{X} is any semi-inner product space and \mathcal{X}_e is its extension, there exists a constant $\kappa > 0$ and a function $\beta(\mathbf{x}_0)$ such that

$$\|(\mathcal{G}(\mathbf{u}))_T\|_{\mathcal{X}} \leq \kappa \|\mathbf{u}_T\|_{\mathcal{X}} + \beta(\mathbf{x}_0) \quad (3)$$

where $\|\cdot\|_{\mathcal{X}}$ is the induced norm of the innerproduct space. If the space \mathcal{X} is \mathcal{L}_2 , then IO stability is called \mathcal{L}_2 stability.

The properties of $(\mathbf{Q}, \mathbf{S}, \mathbf{R})$ of dissipative systems are closely related to the \mathcal{L}_2 -stability through Theorem 1.

Theorem 1. The operator is \mathcal{L}_2 stable if and only if it is *QSR*-dissipative with $\mathbf{Q} \prec 0$.

Dissipativity serves as a powerful framework for \mathcal{L}_2 -stability analysis of large-scale, multi-agent systems.

Theorem 2. (NDT, [Moylan and Hill, 2003]). Consider N dissipative operators, $\mathcal{G}_i : \mathcal{L}_{2e}^{m_i} \mapsto \mathcal{L}_{2e}^{l_i}$ with parameters $(\mathbf{Q}_i, \mathbf{S}_i, \mathbf{R}_i)$, interconnected by the operators, $\mathcal{H}_{ij} : \mathcal{L}_{2e}^{l_j} \mapsto \mathcal{L}_{2e}^{m_i}$, mapping the output of the j^{th} operator to the input of i^{th} operator and represented by matrices $\mathbf{H}_{ij} \in \mathbb{R}^{m_i \times l_j}$. Thereby, the large-scale interconnected system is expressed by

$$\mathbf{y}_i = \mathcal{G} \mathbf{e}_i, \quad \mathbf{y} = \mathcal{G} \mathbf{u}, \quad \mathbf{e} = \mathbf{u} + \mathbf{H} \mathbf{y} \quad (4)$$

where $\mathbf{u} = \text{col}(\mathbf{u}_i)_{i \in \mathbb{N}_N}$, $\mathbf{y} = \text{col}(\mathbf{y}_i)_{i \in \mathbb{N}_N}$, $\mathbf{e} = \text{col}(\mathbf{e}_i)_{i \in \mathbb{N}_N}$, and $\mathcal{G} = \text{diag}(\mathcal{G}_i)_{i \in \mathbb{N}_N}$. Then, $\mathcal{G} : \mathcal{L}_{2e}^m \mapsto \mathcal{L}_{2e}^l$ is \mathcal{L}_2 stable if $\widehat{\mathbf{Q}} \prec 0$, where

$$\widehat{\mathbf{Q}} = \mathbf{Q} + \mathbf{S} \mathbf{H} + \mathbf{H}^T \mathbf{S}^T + \mathbf{H}^T \mathbf{R} \mathbf{H} \quad (5)$$

with $\mathbf{Q} = \text{diag}(\mathbf{Q}_i)_{i \in \mathbb{N}_N}$, and \mathbf{S} and \mathbf{R} defined analogously.

2.3 Convex Overbounding

Optimal controller synthesis minimizes an objective function subject to matrix inequality constraints that are typically bilinear matrix inequality (BMI), expressed as

$$\mathbf{Q} + \text{He}(\mathbf{X} \mathbf{N} \mathbf{Y}) \prec 0, \quad (6)$$

where $\mathbf{N} \in \mathbb{R}^{p \times q}$ is a given matrix, and $\mathbf{Q} \in \mathbb{S}^n$, $\mathbf{X} \in \mathbb{R}^{n \times p}$, and $\mathbf{Y} \in \mathbb{R}^{q \times n}$ are design variables. Since Equation 6 is generally nonconvex, the associated optimal control problem becomes NP-hard. Conservative convex relaxations of Equation 6 can be derived using the following results.

Theorem 3. ([Sebe, 2018], [Ren et al., 2021]). Consider the matrices $\mathbf{Q} \in \mathbb{S}^n$, $\mathbf{N} \in \mathbb{R}^{p \times q}$, $\mathbf{X} \in \mathbb{R}^{n \times p}$, and $\mathbf{Y} \in \mathbb{R}^{q \times n}$, where \mathbf{Q} , \mathbf{X} , and \mathbf{Y} are design variables. The BMI condition $\mathbf{Q} + \text{He}(\mathbf{X} \mathbf{N} \mathbf{Y}) \prec 0$ is implied by either

$$\begin{bmatrix} \mathbf{Q} & \mathbf{X} \mathbf{N} + \mathbf{Y}^T \mathbf{G}^T \\ \mathbf{N}^T \mathbf{X}^T + \mathbf{G} \mathbf{Y} & -\text{He}(\mathbf{G}) \end{bmatrix} \prec 0 \quad (7)$$

for any $\mathbf{G} \in \mathbb{R}^{q \times p}$ satisfying $\text{He}(\mathbf{G}) \succ 0$, or

$$\begin{bmatrix} \mathbf{Q} & * & * & \mathbf{0} \\ \mathbf{N}^T \mathbf{X}^T + \mathbf{G}^0 \mathbf{Y} & -\text{He}(\mathbf{G}^0 + \delta \mathbf{G}) & \mathbf{0} & * \\ \mathbf{Y} & \mathbf{0} & -\mathbf{F} & 0 \\ \mathbf{0} & \mathbf{F}^0 \delta \mathbf{G}^T & \mathbf{0} & -2\mathbf{F}^0 + \mathbf{F} \end{bmatrix} \prec 0 \quad (8)$$

for given $\mathbf{G}^0 \in \mathbb{R}^{q \times p}$ such that $\text{He}(\mathbf{G}^0) \prec 0$ and $\mathbf{F}^0 \in \mathbb{S}^q$, where $\delta \mathbf{G}$ and \mathbf{F} are additional design variables.

Directly applying Theorem 3 may introduce excessive conservatism, making it difficult to obtain a feasible solution to Equation 6. Fortunately, its conservatism can be significantly reduced by linearizing around a feasible point, \mathbf{X}^0 and \mathbf{Y}^0 satisfying $\mathbf{Q} + \text{He}(\mathbf{X}^0 \mathbf{N} \mathbf{Y}^0) \prec 0$, if one is known. Specifically, Theorem 3 can be reformulated by substituting \mathbf{Q} , \mathbf{X} , and \mathbf{Y} with $\mathbf{Q} + \text{He}(\mathbf{X}^0 \mathbf{N} \mathbf{Y}^0 + \delta \mathbf{X} \mathbf{N} \mathbf{Y}^0 + \mathbf{X}^0 \mathbf{N} \delta \mathbf{Y})$, $\delta \mathbf{X}$, and $\delta \mathbf{Y}$, and solve Equation 7 or 8 with new design variables \mathbf{Q} , $\delta \mathbf{X}$, and $\delta \mathbf{Y}$. The resulting problem is always feasible since $\delta \mathbf{X} = \mathbf{0}$ and $\delta \mathbf{Y} = \mathbf{0}$ yields the initial feasible point $(\mathbf{X}^0, \mathbf{Y}^0)$.

3 Sparsity-Promoting Dissipativity-Augmented Control

Consider a plant $\mathcal{G} : \mathbf{u} \rightarrow \mathbf{x}$, where \mathbf{u} and \mathbf{x} are the input and state. The plant is controlled by a full-state feedback controller $\mathcal{C} : \hat{\mathbf{u}} \rightarrow \hat{\mathbf{y}}$, expressed as $\hat{\mathbf{y}} = -\mathbf{K} \hat{\mathbf{u}}$. Disturbances may

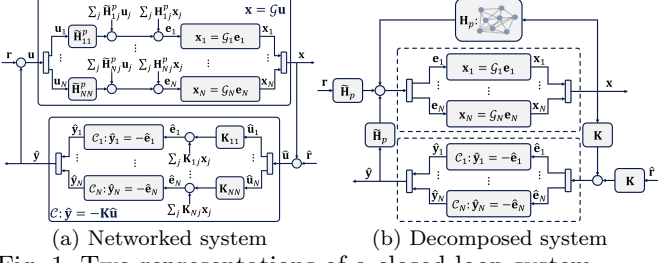


Fig. 1. Two representations of a closed-loop system.

influence both the plant and controller inputs, denoted by \mathbf{r} and $\hat{\mathbf{r}}$, respectively, so that $\mathbf{u} = \mathbf{r} + \hat{\mathbf{y}}$ and $\hat{\mathbf{u}} = \hat{\mathbf{r}} + \mathbf{x}$, respectively. Suppose that the feedback interconnection of \mathcal{G} and \mathcal{C} can be decomposed into: N agents, $\mathcal{G}_i: \mathbf{e}_i \rightarrow \mathbf{x}_i$, where \mathbf{e}_i and \mathbf{x}_i are the input and state of the i^{th} agent; their local controllers, $\mathcal{C}_i: \hat{\mathbf{e}}_i \rightarrow \hat{\mathbf{y}}_i$, expressed as $\hat{\mathbf{y}}_i = -\hat{\mathbf{e}}_i$; and their interconnection gains. The interconnection between the agents and their controller is given by

$$\mathbf{e}_i = \sum_{j \in \mathbb{N}_N, i \neq j} \mathbf{H}_{ij}^p \mathbf{x}_j + \sum_{j \in \mathbb{N}_N} \tilde{\mathbf{H}}_{ij}^p \mathbf{u}_j, \quad \hat{\mathbf{e}}_i = \sum_{j \in \mathbb{N}_N} \mathbf{K}_{ij} \hat{\mathbf{u}}_{ij},$$

$$\begin{bmatrix} \mathbf{e} \\ \hat{\mathbf{e}} \end{bmatrix} = \begin{bmatrix} \mathbf{H}_p & \tilde{\mathbf{H}}_p \\ \mathbf{K} & \mathbf{0} \end{bmatrix} \begin{bmatrix} \mathbf{x} \\ \hat{\mathbf{y}} \end{bmatrix} = \mathbf{H} \begin{bmatrix} \mathbf{x} \\ \hat{\mathbf{y}} \end{bmatrix},$$

where $\mathbf{e} = \text{col}(\mathbf{e}_i)_{i \in \mathbb{N}_N}$, and $\hat{\mathbf{e}}$, \mathbf{x} , and $\hat{\mathbf{y}}$ are defined analogously. \mathbf{H}_p characterizes the interconnection structure among agent, $\tilde{\mathbf{H}}_p$ represents the interconnection structure from the input of the plant to the input of each agent, and \mathbf{H}_{ij}^p and $\tilde{\mathbf{H}}_{ij}^p$ are the corresponding block components. Figure 1 depicts this system decomposition. The objective is to synthesize a sparse controller \mathbf{K} that stabilizes the overall interconnected system in the presence of disturbances \mathbf{r} and $\hat{\mathbf{r}}$, while minimizing a standard LQ criterion.

3.1 Dual-Model Synthesis

Stability is ensured by enforcing *QSR*-dissipativity properties on each agent and its local controller, \mathcal{G}_i and \mathcal{C}_i , and by applying Theorem 2. Although the external inputs to the decomposed network are $\tilde{\mathbf{H}}_p \mathbf{r}$ and $\mathbf{K} \hat{\mathbf{r}}$, Theorem 2 remains applicable because signals remain in \mathcal{L}_2 after premultiplication by a constant gain.

The LQ criterion is evaluated based on the closed-loop dynamics of the linearized plant, \mathcal{G}^{LTI} , and controller, described as

$$\mathcal{G}^{LTI}: \dot{\mathbf{x}} = \mathbf{A}\mathbf{x} + \mathbf{B}\mathbf{u}, \quad \mathcal{C}: \mathbf{u} = -\mathbf{K}\mathbf{x},$$

where \mathbf{A} and \mathbf{B} denote the linearized system matrices of the plant. Synthesizing \mathbf{K} matrix that minimizes LQ criterion of the closed-loop system is equivalent to solving

$$\begin{aligned} & \arg \min_{\mathbf{K}, \mathbf{P}} \text{Trace}(\mathbf{P}) \\ & \text{s.t. } \text{He}(\mathbf{P}(\mathbf{A} - \mathbf{B}\mathbf{K})) + \mathbf{Q}_{lq} + \mathbf{K}^T \mathbf{R}_{lq} \mathbf{K} \preceq 0, \quad \mathbf{P} \succ 0 \end{aligned}$$

where $\mathbf{Q}_{lq} \succ 0$ and $\mathbf{R}_{lq} \succ 0$ are state and control weight of the LQ criterion [Khalil et al., 1996]. To promote the sparsity in \mathbf{K} , a penalty function $g(\mathbf{K})$ is incorporated into the objective function. Typical sparsity-promoting penalty functions include the ℓ_1 norm, weighted ℓ_1 norm, sum-of-logs, and the cardinality function of \mathbf{K} [Lin et al., 2013].

In conclusion, the sparsity-promoting dissipativity-augmented controller is obtained by solving

$$\arg \min_{\mathbf{K}, \mathbf{P}} \text{Trace}(\mathbf{P}) + \gamma g(\mathbf{K}) \quad (9a)$$

$$\text{s.t. } \text{He}(\mathbf{P}(\mathbf{A} - \mathbf{B}\mathbf{K})) + \mathbf{Q}_{lq} + \mathbf{K}^T \mathbf{R}_{lq} \mathbf{K} \preceq 0, \quad \mathbf{P} \succ 0, \quad (9b)$$

$$\int_0^T \begin{bmatrix} \mathbf{y}_i \\ \mathbf{e}_i \end{bmatrix}^T \begin{bmatrix} \mathbf{Q}_i & \mathbf{S}_i \\ * & \mathbf{R}_i \end{bmatrix} \begin{bmatrix} \mathbf{y}_i \\ \mathbf{e}_i \end{bmatrix} dt \geq 0, \quad \forall i \in \mathbb{N}_N, \quad (9c)$$

$$-\hat{\mathbf{R}}_i + \text{He}(\hat{\mathbf{S}}_i) - \hat{\mathbf{Q}}_i \preceq 0, \quad \forall i \in \mathbb{N}_N, \quad (9d)$$

$$\mathbf{Q} + \text{He}(\mathbf{S}\mathbf{H}) + \mathbf{H}^T \mathbf{R}\mathbf{H} \prec 0. \quad (9e)$$

where γ denotes a penalty parameter, $(\mathbf{Q}_i, \mathbf{S}_i, \mathbf{R}_i)$ and $(\hat{\mathbf{Q}}_i, \hat{\mathbf{S}}_i, \hat{\mathbf{R}}_i)$ respectively represents *QSR* parameters of i^{th} agent and its local controller, and $\mathbf{Q} = \text{diag}(\text{diag}(\mathbf{Q}_i)_{i \in \mathbb{N}_N}, \text{diag}(\hat{\mathbf{Q}}_i)_{i \in \mathbb{N}_N})$, while \mathbf{S} and \mathbf{R} are defined analogously. However, Equation 9 is non-convex optimization problem, due to Equation 9b, 9c and 9e. These constraints are relaxed to linear matrix inequalities in Section 4.

4 Main Results

In this section, the strategies solving Equation 9 are proposed. A convex relaxation of Equation 9 is presented to obtain a feasible solution in a computationally tractable manner. Equation 9c is reformulated to linear matrix inequalities (LMIs) by applying the expansions from Lemma 1, based on the structures of agents. Equation 9b and 9e are reconstructed using the convex overbounding techniques introduced in Section 2.3. Section 4.4 provides the approach to compute a feasible sparse controller than improves the LQ performance criterion, based on ADMM.

4.1 Agent Dissipativity

Definition 1 cannot be directly applied to solve Equation 9 using the existing semidefinite programming (SDP)-based optimization solvers. Fortunately, many variations of Definition 1 result in tractable LMIs that enforce the *QSR*-dissipativity of certain nonlinear systems. For agents \mathcal{G}_i modeled as LTI systems, Lemma 1 can be applied to impose the dissipativity constraint. If \mathcal{G}_i is an LTI system with polytopic uncertainty in its dynamics, [Walsh and Forbes, 2019, Equation 18] can be used to verify the *QSR*-dissipativity of the agent. In case where \mathcal{G}_i an LTI system with time delays in its input, output, and state, the results in [Bridgeman and Forbes, 2016, Theorem 3.1] provides an LMI condition for determining dissipativity parameters of the agent.

If no existing LMI condition ensures the dissipativity of \mathcal{G}_i , the predefined dissipativity parameters $(\mathbf{Q}_i^p, \mathbf{S}_i^p, \mathbf{R}_i^p)$ can be used together with a scalar design variable λ , such that $\mathbf{Q}_i = \lambda \mathbf{Q}_i^p$, $\mathbf{S}_i = \lambda \mathbf{S}_i^p$, and $\mathbf{R}_i = \lambda \mathbf{R}_i^p$. Although these parameters are fixed, introducing the scalar variable λ alleviates the conservatism inherent in the fixed characterizations. Various approaches exist to find the dissipativity of nonlinear agents. For instance, agents following Euler-Lagrange systems is passive, meaning $\mathbf{Q}_i^p = \mathbf{0}$, $\mathbf{S}_i^p = \frac{1}{2} \mathbf{I}$, and $\mathbf{R}_i^p = \mathbf{0}$ [Lozano et al., 2013, Chapter 6]. In addition, data-driven methods such as [Romer et al., 2017] can be employed to estimate $(\mathbf{Q}_i^p, \mathbf{S}_i^p, \mathbf{R}_i^p)$ for the agents.

4.2 Convex Overbounding of BMI Constraints

Convexification tricks in Theorem 3 can be applied to yield LMIs implying Equation 9b and 9e, explained in Corollary 1 and 2.

Corollary 1. Suppose that \mathbf{K}^0 and \mathbf{P}^0 are feasible points of Equation 9b. For any \mathbf{G}^0 and \mathbf{F}^0 satisfying $\text{He}(\mathbf{G}^0) \succeq 0$ and $\mathbf{F}^0 \succeq 0$,

$$\begin{bmatrix} \mathbf{L} + \mathbf{Q}_{lq} & * & * & * & \mathbf{0} \\ \mathbf{K}^0 + \delta\mathbf{K} & -\mathbf{R}_{lq}^{-1} & \mathbf{0} & \mathbf{0} & \mathbf{0} \\ (\mathbf{B}\delta\mathbf{P})^T - \mathbf{G}^0\delta\mathbf{K} & \mathbf{0} & -\text{He}(\mathbf{G}^0 + \delta\mathbf{G}) & \mathbf{0} & * \\ -\delta\mathbf{K} & \mathbf{0} & \mathbf{0} & -\mathbf{F} & \mathbf{0} \\ \mathbf{0} & \mathbf{0} & \mathbf{F}^0\delta\mathbf{G}^T & \mathbf{0} & -2\mathbf{F}^0 + \mathbf{F} \end{bmatrix} \preceq 0, \quad (10)$$

where $\mathbf{L} = \text{He}((\mathbf{P}^0 + \delta\mathbf{P})(\mathbf{A} - \mathbf{B}\mathbf{K}^0) - \delta\mathbf{P}\mathbf{B}\mathbf{K}^0)$, implies that $\mathbf{K}^0 + \delta\mathbf{K}$ and $\mathbf{P}^0 + \delta\mathbf{P}$ are feasible solution of Equation 9b.

Proof. The proof follows by applying Schur complement and the overbounding condition in Equation 8 of Theorem 3. Since $\mathbf{R}_{lq} \succ 0$, applying Schur complement to Equation 9b and substituting \mathbf{K} and \mathbf{P} with $\mathbf{K}^0 + \delta\mathbf{K}$ and $\mathbf{P}^0 + \delta\mathbf{P}$ yield

$$\begin{bmatrix} \mathbf{L} + \mathbf{Q}_{lq} & * \\ \mathbf{K}^0 + \delta\mathbf{K} & -\mathbf{R}_{lq}^{-1} \end{bmatrix} + \text{He} \left(\begin{bmatrix} \delta\mathbf{P}\mathbf{B} \\ \mathbf{0} \end{bmatrix} \begin{bmatrix} -\delta\mathbf{K} & \mathbf{0} \end{bmatrix} \right) \preceq 0$$

which is equivalent to Equation 9b. Next, applying Equation 8 in Theorem 3 with $\mathbf{X} = [(\delta\mathbf{P}\mathbf{B})^T \mathbf{0}]^T$, $\mathbf{Y} = [-\delta\mathbf{K} \mathbf{0}]$, and $\mathbf{N} = \mathbf{I}$ yields Equation 10. ■

Corollary 2. Suppose that $\mathbf{Q}^0, \mathbf{S}^0, \mathbf{R}^0$, and \mathbf{H}^0 are feasible points of Equation 9e. Then

$$\begin{bmatrix} \mathbf{M} & * & * & * \\ \delta\mathbf{S}^T + \delta\mathbf{H} & -2\mathbf{I} & \mathbf{0} & \mathbf{0} \\ \frac{1}{2}\mathbf{R}^0\delta\mathbf{H} + \delta\mathbf{H} & \mathbf{0} & -2\mathbf{I} & * \\ \delta\mathbf{R}\mathbf{H}^0 + \delta\mathbf{H} & \mathbf{0} & \frac{1}{2}\delta\mathbf{R} & -2\mathbf{I} \end{bmatrix} \prec 0 \quad (11)$$

where $\mathbf{M} = \mathbf{Q}^0 + \delta\mathbf{Q} + \text{He}(\mathbf{S}^0\mathbf{H}^0 + \delta\mathbf{S}\mathbf{H}^0 + \mathbf{S}^0\delta\mathbf{H}) + \mathbf{H}^{0T}\mathbf{R}^0\mathbf{H}^0 + \mathbf{H}^{0T}\delta\mathbf{R}\mathbf{H}^0 + \text{He}(\delta\mathbf{H}^T\mathbf{R}^0\mathbf{H}^0)$, implies that $\mathbf{Q}^0 + \delta\mathbf{Q}$, $\mathbf{S}^0 + \delta\mathbf{S}$, $\mathbf{R}^0 + \delta\mathbf{R}$, and $\mathbf{H}^0 + \delta\mathbf{H}$ are feasible solution of Equation 9e.

Proof. Since Equation 9e is a trilinear matrix inequality and $\mathbf{R} \not\succ 0$, Equation 11 is obtained by applying Equation 7 of Theorem 3 twice to Equation 9e. First, using $\mathbf{S} = \mathbf{S}^0 + \delta\mathbf{S}$ and $\mathbf{H} = \mathbf{H}^0 + \delta\mathbf{H}$ allows Equation 9e to be reformulated as

$$\begin{aligned} & \mathbf{Q} + \text{He}(\mathbf{S}^0\mathbf{H}^0 + \delta\mathbf{S}\mathbf{H}^0 + \mathbf{S}^0\delta\mathbf{H}) + \mathbf{H}^{0T}\mathbf{R}\mathbf{H}^0 + \text{He}(\delta\mathbf{H}^T\mathbf{R}\mathbf{H}^0) \\ & + \text{He} \left(\begin{bmatrix} \delta\mathbf{S} & \frac{1}{2}\delta\mathbf{H}^T\mathbf{R} \end{bmatrix} \begin{bmatrix} \delta\mathbf{H} \\ \mathbf{0} \end{bmatrix} \right) \prec 0 \end{aligned}$$

Applying Equation 7 of Theorem 3 with $\mathbf{X} = [\delta\mathbf{S} \frac{1}{2}\delta\mathbf{H}^T\mathbf{R}]$, $\mathbf{Y} = [\delta\mathbf{H}^T \delta\mathbf{H}^T]^T$, $\mathbf{N} = \mathbf{I}$ and $\mathbf{G} = \mathbf{I}$, and replacing \mathbf{Q} and \mathbf{R} with $\mathbf{Q}^0 + \delta\mathbf{Q}$ and $\mathbf{R}^0 + \delta\mathbf{R}$, respectively, lead to

$$\begin{bmatrix} \mathbf{M} & * & * \\ \delta\mathbf{S}^T + \delta\mathbf{H} & -2\mathbf{I} & \mathbf{0} \\ \frac{1}{2}\mathbf{R}^0\delta\mathbf{H} + \delta\mathbf{H} & \mathbf{0} & -2\mathbf{I} \end{bmatrix} + \text{He} \left(\begin{bmatrix} \mathbf{H}^{0T}\delta\mathbf{R} \\ \mathbf{0} \\ \frac{1}{2}\delta\mathbf{R} \end{bmatrix} \begin{bmatrix} \delta\mathbf{H} & \mathbf{0} & \mathbf{0} \end{bmatrix} \right) \prec 0$$

Finally, applying Equation 7 of Theorem 3 once more with $\mathbf{X} = [\delta\mathbf{R}^T\mathbf{H}^0 \mathbf{0} \frac{1}{2}\delta\mathbf{R}^T]^T$, $\mathbf{Y} = [\delta\mathbf{H} \mathbf{0} \mathbf{0}]$, $\mathbf{N} = \mathbf{I}$, and $\mathbf{G} = \mathbf{I}$ results in Equation 11. ■

For the application of Corollary 2 to Equation 9e, the design variables are defined as

$$\delta\mathbf{H} = \begin{bmatrix} \mathbf{0} & \mathbf{0} \\ \delta\mathbf{K} & \mathbf{0} \end{bmatrix}, \quad \delta\mathbf{Q} = \begin{bmatrix} \text{diag}(\delta\mathbf{Q}_i)_{i \in \mathbb{N}_N} & \mathbf{0} \\ \mathbf{0} & \text{diag}(\delta\widehat{\mathbf{Q}}_i)_{i \in \mathbb{N}_N} \end{bmatrix},$$

and $\delta\mathbf{S}$ and $\delta\mathbf{R}$ are defined likewise. Applying Corollary 1 and 2, we have the problem

$$\arg \min_{\delta\mathbf{K}, \delta\mathbf{P}, \delta\mathbf{Q}, \delta\mathbf{S}, \delta\mathbf{R}, \delta\mathbf{G}, \mathbf{F}} \text{Trace}(\mathbf{P}^0 + \delta\mathbf{P}) \quad (12a)$$

$$\text{s.t. } \mathbf{N}(\delta\mathbf{Q}, \delta\mathbf{S}, \delta\mathbf{R}, \delta\mathbf{K}, \delta\mathbf{P}, \delta\mathbf{G}, \mathbf{F}) \preceq 0, \quad (12b)$$

to construct the centralized controller for given initial feasible point, where $\mathbf{N}(\delta\mathbf{Q}, \delta\mathbf{S}, \delta\mathbf{R}, \delta\mathbf{K}, \delta\mathbf{P}, \delta\mathbf{G}, \mathbf{F})$ denotes the block diagonal composition of all matrices associated with the LMIs.

4.3 Initialization

Initial feasible points of Equation 9 or 12, denoted by \mathbf{P}^0 , \mathbf{K}^0 , \mathbf{Q}^0 , \mathbf{S}^0 , \mathbf{R}^0 , $\widehat{\mathbf{Q}}^0$, $\widehat{\mathbf{S}}^0$, $\widehat{\mathbf{R}}^0$, \mathbf{G}^0 , and \mathbf{F}^0 , are required to solve Equation 12. Heuristically, localized controllers $\mathbf{K}_i \in \mathbb{R}$ for $i \in \mathbb{N}_N$ can be initialized based on classical control methods, such as PD control, and a feasible point of Equation 9 can then be obtained with these fixed local controllers. If the constraints are not satisfied for a chosen localized controller, the feasibility check is repeated with increased controller gains until a feasible point is found. Once a feasible set of local controller is obtained, solving Equation 12 results in the initial feasible point corresponding to a centralized initial controller. Alternatively, the iterative relaxation strategy proposed in [Warner and Scruggs, 2017] can also be employed to obtain an initial feasible solution. For \mathbf{G}^0 and \mathbf{F}^0 , any matrices satisfying conditions in Corollary 1 can be used, and \mathbf{I} is commonly used for the initialization.

4.4 Sparsity Promotion

Once the initial centralized feasible points are obtained, the optimal sparse structure can be determined by

$$\arg \min_{\delta\mathbf{K}, \delta\mathbf{P}, \delta\mathbf{Q}, \delta\mathbf{S}, \delta\mathbf{R}, \delta\mathbf{G}, \mathbf{F}} \text{Trace}(\mathbf{P}^0 + \delta\mathbf{P}) + \gamma g(\mathbf{K}^0 + \delta\mathbf{K}) \quad (13a)$$

$$\text{s.t. } \mathbf{N}(\delta\mathbf{Q}, \delta\mathbf{S}, \delta\mathbf{R}, \delta\mathbf{K}, \delta\mathbf{P}, \delta\mathbf{G}, \mathbf{F}) \preceq 0, \quad (13b)$$

where a penalty function $g(\mathbf{K}^0 + \delta\mathbf{K})$ is introduced to promote sparsity in the feedback gain. Several forms can be considered as the penalty function. In this work, the cardinality function and weighted ℓ_1 norm are employed, since the weighted ℓ_1 norm provides an appropriate convex approximation of the cardinality penalty [Lin et al., 2013].

The weighted ℓ_1 norm is defined as

$$g(\mathbf{K}^0 + \delta\mathbf{K}) = \sum_{i,j \in \mathbb{N}_N} W_{ij} \|\mathbf{K}_{ij}^0 + \delta\mathbf{K}_{ij}\|_F \quad (14)$$

where W_{ij} are non-negative weight. If W_{ij} are inversely proportional to $\|\mathbf{K}_{ij}^0 + \delta\mathbf{K}_{ij}\|_F$, the weighted ℓ_1 norm becomes equivalent to the cardinality penalty. However, this exact formulation cannot be implemented, since W_{ij} depend on the unknown variables [Lin et al., 2013]. Instead, the structure of the initial feasible controller \mathbf{K}^0 can be used to define W_{ij} as $\|\mathbf{K}_{ij}^0\|_F^{-1}$ when $\|\mathbf{K}_{ij}^0\|_F \neq 0$ or ϵ_l^{-1} otherwise. When this weighted ℓ_1 norm is used, the penalty function becomes convex, allowing Equation 13 to be solved directly by standard optimization solvers without relying on specialized algorithms.

Lin et al. [2013] proposed solving the problem with cardinality penalty using the ADMM algorithm. Although ADMM does not guarantee convergence for nonconvex

objectives, extensive computational experience has shown that it performs well in practice when the augmented Lagrangian parameter is sufficiently large [Boyd et al., 2011].

The same strategy in Lin et al. [2013] is applied to Equation 13 using cardinality penalty function

$$g(\mathbf{K}^0 + \delta\mathbf{K}) = \sum_{i \in \mathbb{N}_N} \sum_{j \in \mathbb{N}_N} \text{card} \left(\|\mathbf{K}_{ij}^0 + \delta\mathbf{K}_{ij}\|_F \right). \quad (15)$$

By introducing the indicator function $I_{\mathbf{N}}$ and an auxiliary variable \mathbf{Z} , where $I_{\mathbf{N}}$ takes 0 if $\mathbf{N} \preceq 0$ and $+\infty$ otherwise, Equation 13 is equivalently written as

$$\begin{aligned} \arg \min_{\substack{\delta\mathbf{K}, \delta\mathbf{P}, \mathbf{Z}, \delta\mathbf{G} \\ \delta\mathbf{Q}, \delta\mathbf{S}, \delta\mathbf{R}, \mathbf{F}}} & J(\delta\mathbf{P}) + I_{\mathbf{N}}(\delta\mathbf{Q}, \delta\mathbf{S}, \delta\mathbf{R}, \delta\mathbf{K}, \delta\mathbf{P}, \delta\mathbf{G}, \mathbf{F}) + \gamma g(\mathbf{Z}) \\ \text{s.t. } & \mathbf{K}^0 + \delta\mathbf{K} - \mathbf{Z} = 0, \end{aligned}$$

where $J(\delta\mathbf{P}) = \text{Trace}(\mathbf{P}^0 + \delta\mathbf{P})$. The goal of ADMM is to solve

$$\begin{aligned} \arg \min_{\substack{\delta\mathbf{K}, \delta\mathbf{P}, \mathbf{Z}, \delta\mathbf{G} \\ \delta\mathbf{Q}, \delta\mathbf{S}, \delta\mathbf{R}, \mathbf{F}}} & J(\delta\mathbf{P}) + I_{\mathbf{N}}(\delta\mathbf{Q}, \delta\mathbf{S}, \delta\mathbf{R}, \delta\mathbf{K}, \delta\mathbf{P}, \delta\mathbf{G}, \mathbf{F}) + \gamma g(\mathbf{Z}) \\ & + \text{Trace}(\mathbf{\Lambda}^T(\mathbf{K}^0 + \delta\mathbf{K} - \mathbf{Z})) + \frac{\rho}{2} \|\mathbf{K}^0 + \delta\mathbf{K} - \mathbf{Z}\|_F^2 \end{aligned}$$

by iteratively solving

$$\begin{aligned} \delta\mathbf{K}^{k+1} = \arg \min_{\substack{\delta\mathbf{K}, \delta\mathbf{P}, \delta\mathbf{Q}, \\ \delta\mathbf{S}, \delta\mathbf{R}, \delta\mathbf{G}, \mathbf{F}}} & \text{Trace}(\mathbf{P}^0 + \delta\mathbf{P}) + \frac{\rho}{2} \|\mathbf{K}^0 + \delta\mathbf{K} - \mathbf{Z}^k + \mathbf{\Lambda}^k\|_F^2 \\ \text{s.t. } & \mathbf{N}(\delta\mathbf{Q}, \delta\mathbf{S}, \delta\mathbf{R}, \delta\mathbf{K}, \delta\mathbf{P}, \delta\mathbf{G}, \mathbf{F}) \preceq 0, \end{aligned} \quad (16a)$$

$$\mathbf{Z}^{k+1} = \arg \min_{\mathbf{Z}} \gamma g(\mathbf{Z}) + \frac{\rho}{2} \|\mathbf{K}^0 + \delta\mathbf{K}^{k+1} - \mathbf{Z} + \mathbf{\Lambda}^k\|_F^2, \quad (16b)$$

$$\mathbf{\Lambda}^{k+1} = \mathbf{\Lambda}^k + (\mathbf{K}^0 + \delta\mathbf{K}^{k+1} - \mathbf{Z}^{k+1}), \quad (16c)$$

where $\mathbf{\Lambda}$ is the dual variable, k is the iteration index, $\rho > 0$ is the augmented Lagrangian parameter. If Equation 15 is used as the penalty, the block component of the unique solution of Equation 16b is

$$\mathbf{Z}_{ij}^{k+1} = \begin{cases} \mathbf{V}_{ij}, & \|\mathbf{V}_{ij}\|_F > \sqrt{\frac{2\gamma}{\rho}} \\ \mathbf{0}, & \text{o.w.} \end{cases}$$

where $\mathbf{V} = \mathbf{K}^0 + \delta\mathbf{K}^{k+1} + \mathbf{\Lambda}^k$ [Lin et al., 2013]. The stopping criteria of ADMM are

$$r_p = \frac{\|\mathbf{K}^0 + \delta\mathbf{K}^k - \mathbf{Z}^k\|_F}{\|\mathbf{Z}^k\|_F} \leq \epsilon_p \text{ and } r_d = \frac{\|\mathbf{Z}^k - \mathbf{Z}^{k-1}\|_F}{\|\mathbf{Z}^k\|_F} \leq \epsilon_d.$$

After solving Equation 13, the controller is updated to $\mathbf{K}_1 = \mathbf{K}^0 + \delta\mathbf{K}^*$, where $\delta\mathbf{K}^*$ is the optimal perturbation obtained from the solution. The matrices $\mathbf{Q}^1, \mathbf{S}^1, \mathbf{R}^1, \widehat{\mathbf{Q}}^1, \widehat{\mathbf{S}}^1, \widehat{\mathbf{R}}^1, \mathbf{Y}^1$, and \mathbf{G}^1 are updated accordingly, and $\mathbf{F}^1 = \mathbf{F}^*$. The subspace \mathcal{K} is then defined as the set of block matrices that share the same sparsity pattern as \mathbf{K}^1 .

4.5 Structured ICO

The process described in Section 4.4 results in the solution of Equation 13, which represents a linear convex relaxation of Equation 9 obtained by linearizing around the initial feasible points. This implies that the resulting solutions are not necessarily local optima of Equation 9. Intuitively, the closed-loop performance can be further improved by iteratively solving Equation 13 by using the feasible points obtained from the previous iteration as the initial points. However, such an approach does not preserve the convergence guarantees of ICO, since the cardinality operator is pointwise discontinuous at zero, and no approximation of the cardinality can simultaneously be an

Algorithm 1 Sparsity-Promoting Dissipativity-Augmented Controller Synthesis

Input: $g, \mathbf{Y}^0, \mathbf{K}^0, \mathbf{Q}^0, \mathbf{S}^0, \mathbf{R}^0, \widehat{\mathbf{Q}}^0, \widehat{\mathbf{S}}^0, \widehat{\mathbf{R}}^0, \mathbf{G}^0, \mathbf{F}^0, \epsilon_p, \epsilon_d, \epsilon$
Outputs: \mathbf{K}

- 1: **if** $g(\mathbf{K}^0 + \delta\mathbf{K})$ follows Equation 14 **then**
- 2: Find $\delta\mathbf{K}^*$ by solving Equation 13
- 3: **else if** $g(\mathbf{K}^0 + \delta\mathbf{K})$ follows Equation 15 **then**
- 4: **while** $r_p > \epsilon_p$ or $r_d > \epsilon_d$ **do**
- 5: Find $\delta\mathbf{K}^{k+1}$ by solving Equation 16a
- 6: Find \mathbf{Z}^{k+1} by solving Equation 16b
- 7: Find $\mathbf{\Lambda}^{k+1}$ by solving Equation 16c
- 8: **end while**
- 9: **end if**
- 10: Set $\mathbf{K}^1 = \mathbf{K}^0 + \delta\mathbf{K}^*$, and update corresponding feasible points, $\mathbf{Y}^1, \mathbf{Q}^1, \mathbf{S}^1, \mathbf{R}^1, \widehat{\mathbf{Q}}^1, \widehat{\mathbf{S}}^1, \widehat{\mathbf{R}}^1$, and \mathbf{G}^1 analogous to \mathbf{K}^1 , and set $\mathbf{F}^1 = \mathbf{F}^*$
- 11: Define the structured subspace \mathcal{K} based on the sparsity pattern of \mathbf{K}^1
- 12: **while** $\frac{\text{Trace}(\mathbf{Y}^k) - \text{Trace}(\mathbf{Y}^{k+1})}{\text{Trace}(\mathbf{Y}^{k+1})} > \epsilon$ **do**
- 13: Solve Equation 17 using $\mathbf{K}^k, \mathbf{Y}^k, \mathbf{Q}^k, \mathbf{S}^k, \mathbf{R}^k, \widehat{\mathbf{Q}}^k, \widehat{\mathbf{S}}^k, \widehat{\mathbf{R}}^k, \mathbf{G}^k$, and \mathbf{F}^k
- 14: Set $\mathbf{K}^{k+1} = \mathbf{K}^k + \delta\mathbf{K}^*$, and other feasible points, $\mathbf{Y}^{k+1}, \mathbf{Q}^{k+1}, \mathbf{S}^{k+1}, \mathbf{R}^{k+1}, \widehat{\mathbf{Q}}^{k+1}, \widehat{\mathbf{S}}^{k+1}, \widehat{\mathbf{R}}^{k+1}$, and \mathbf{G}^{k+1} analogous to \mathbf{K}^1 , and set $\mathbf{F}^{k+1} = \mathbf{F}^*$
- 15: **end while**

overbound, convex, and nonconservative at zero [LoCicero and Bridgeman, 2022]. Therefore, instead of iteratively solving Equation 13, we consider

$$\arg \min_{\substack{\delta\mathbf{K}, \delta\mathbf{P}, \delta\mathbf{Q}, \\ \delta\mathbf{S}, \delta\mathbf{R}, \delta\mathbf{G}, \mathbf{F}}} \text{Trace}(\mathbf{P}^k + \delta\mathbf{P}) \quad (17a)$$

$$\text{s.t. } \mathbf{N}(\delta\mathbf{Q}, \delta\mathbf{S}, \delta\mathbf{R}, \delta\mathbf{K}, \delta\mathbf{P}, \delta\mathbf{G}, \mathbf{F}) \preceq 0, \quad (17b)$$

$$\mathbf{K}^k + \delta\mathbf{K} \in \mathcal{K}, \quad (17c)$$

where \mathcal{K} is the subspace achieved from Section 4.4. This problem is used within the ICO framework to iteratively update the feasible points, yielding the optimal sparse controller \mathbf{K}^* . The overall procedure of Section 4 for obtaining \mathbf{K}^* is summarized in Algorithm 1.

4.6 Convergence of Algorithm 1

Algorithm 1 consists of two major stages, sparsity promotion, described in Section 4.4, and ICO, described in Section 4.5. The ICO is always feasible and converges to a local optimum, since it retains at least one feasible point, which is the solution of the previous iteration, and the cost of the problem in each iteration is guaranteed to be no greater than that of this feasible point. In contrast, the convergence behavior of the sparsity-promotion stage depends on the choice of the penalty function. When the weighted ℓ_1 norm is employed, the algorithm converges to a specific structured controller because the problem is formulated as a SDP, which can be solved using standard convex optimization solvers. On the other hand, when the cardinality function is used, there is no convergence guarantee due to its inherent nonconvexity. Nevertheless, extensive computational studies have shown that the ADMM algorithm performs well in practice when the value of ρ is sufficiently large [Boyd et al., 2011].

5 Numerical Examples

In this example, sparse controllers for a networked system composed of $N=10$ agents with uncertain parameters are synthesized using Algorithm 1. The 10 agents are randomly distributed over a 10×10 grid, and their dynamics deviate randomly from their nominal models. The nominal dynamics of each agent follow the model introduced in [Motee and Jadbabaie, 2008], expressed as

$$\dot{\mathbf{x}}_i = \hat{\mathbf{A}}_{ii} \mathbf{x}_i + \sum_{j \neq i} e^{-\alpha(i-j)} \mathbf{x}_j + \begin{bmatrix} 0 \\ 1 \end{bmatrix} \mathbf{e}_i$$

where $\hat{\mathbf{A}}_{ii}$ are given by $\begin{bmatrix} 1 & 1 \\ 1 & 2 \end{bmatrix}$ for $i \in \mathbb{N}_5$ and $\begin{bmatrix} -2 & 1 \\ 1 & -3 \end{bmatrix}$

otherwise, $\alpha=0.1823$, $\mathbf{x}_i \in \mathbb{R}^2$, and $\mathbf{e}_i \in \mathbb{R}$. Hence, the nominal dynamics of the first 5 agents are unstable, whereas those of the remaining five agents are stable. From local dynamics, \mathbf{H}_p is the block matrix where $\mathbf{H}_{ii}^p = \mathbf{0}_{2 \times 2}$ and $\mathbf{H}_{ij}^p = e^{-\alpha(i-j)} \mathbf{I}_2$, and $\tilde{\mathbf{H}}_p = \text{diag}([0 \ 1]^T)_{i \in \mathbb{N}_{10}}$. The linearized system for studying LQ objective is defined using $\mathbf{A} = \text{diag}(\hat{\mathbf{A}}_{ii})_{i \in \mathbb{N}_{10}} + \mathbf{H}$ and $\mathbf{B} = \tilde{\mathbf{H}}_p$.

The actual dynamics \mathbf{A}_{ii} of each agent are uniformly distributed within $\pm 30\%$ of their nominal values $\hat{\mathbf{A}}_{ii}$. Accordingly, each agent's dynamics can be modeled as an LTI system with polytopic uncertainty, represented by a polyhedron with 16 vertices, where each vertex corresponds to the case in which one parameter of \mathbf{A}_{ii} attains either its maximum or minimum value within the uniform distribution. Since some agents are unstable without control, [Walsh and Forbes, 2019, Equation 18] cannot be applied because it requires stability of the open-loop systems. Therefore, Lemma 2 is used, with \mathbf{A}^j denoting the 8 vertices of the polytope and $\mathbf{B}^j = \mathbf{I}_2$ for all $j \in \mathbb{N}_8$.

Lemma 2. The operator $\mathcal{G} : \mathcal{L}_{2e}^m \mapsto \mathcal{L}_{2e}^l$ defined by $\dot{\mathbf{x}}(t) = \mathbf{A}(t)\mathbf{x}(t) + \mathbf{B}(t)\mathbf{u}(t)$ and $\mathbf{y}(t) = \mathbf{x}(t)$, where $\mathbf{A}(t) = \sum_{j=1}^v \zeta_j(t) \mathbf{A}^j$ and $\mathbf{B}(t) = \sum_{j=1}^v \zeta_j(t) \mathbf{B}^j$ with $\sum_{j=1}^v \zeta_j(t) = 1$ for all $t \in \mathbb{R}_+$, is *QSR*-dissipative if there exist a matrix $\mathbf{P} \succ 0$ and matrices \mathbf{Q}, \mathbf{S} , and \mathbf{R} such that

$$\begin{bmatrix} \text{He}(\mathbf{P}\mathbf{A}^j) - \mathbf{Q} \mathbf{P}\mathbf{B}^j - \mathbf{S} \\ (\mathbf{P}\mathbf{B}^j)^T - \mathbf{S}^T & -\mathbf{R} \end{bmatrix} \preceq 0, \quad \forall j \in \mathbb{N}_v \quad (18)$$

Proof. The proof proceeds by verifying Lemma 1. The operator is *QSR* dissipative if Lemma 1 holds for $(\mathbf{A}(t), \mathbf{B}(t), \mathbf{I}, \mathbf{0})$. When $\mathbf{C} = \mathbf{I}$ and $\mathbf{D} = \mathbf{0}$, Equation 2 becomes affine in $\mathbf{A}(t)$ and $\mathbf{B}(t)$. Therefore,

$$\sum_{j=1}^v \zeta_j(t) \begin{bmatrix} \text{He}(\mathbf{P}\mathbf{A}^j) - \mathbf{Q} \mathbf{P}\mathbf{B}^j - \mathbf{S} \\ (\mathbf{P}\mathbf{B}^j)^T - \mathbf{S}^T & -\mathbf{R} \end{bmatrix} \preceq 0$$

Hence, Equation 18 implies Lemma 1 holds for all admissible convex combinations of the polytopic system, establishing *QSR*-dissipativity of the operator \mathcal{G} . \blacksquare

The initial local controller for all agents is set to [1000 100]. To apply Algorithm 1, the parameters are chosen as $\mathbf{Q}_{lq} = 100\mathbf{I}_{20}$, $\mathbf{R}_{lq} = \mathbf{I}_{20}$, $\epsilon_l = 10^{-3}$, $\epsilon_p = \epsilon_d = 10^{-4}$, $\rho = 100$, and $\epsilon = 10^{-3}$. The weighting factor γ is varied from 100 to 300 in increments of 5 for the weighted ℓ_1 norm penalty, and from 335 to 1270 in increments of 5 for the cardinality penalty. For the comparison, the approaches in [Lin et al., 2013; Lian et al., 2018] are implemented for the same system

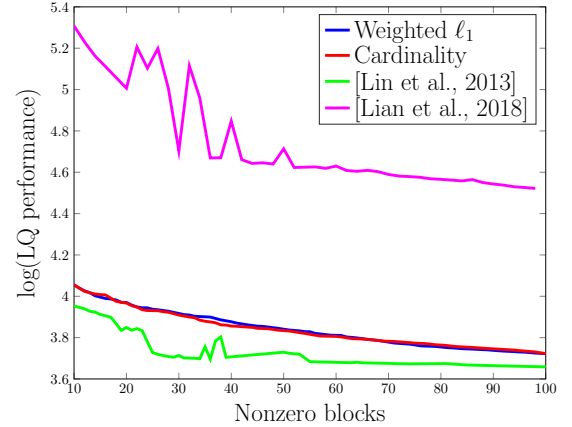


Fig. 2. LQ performance index.

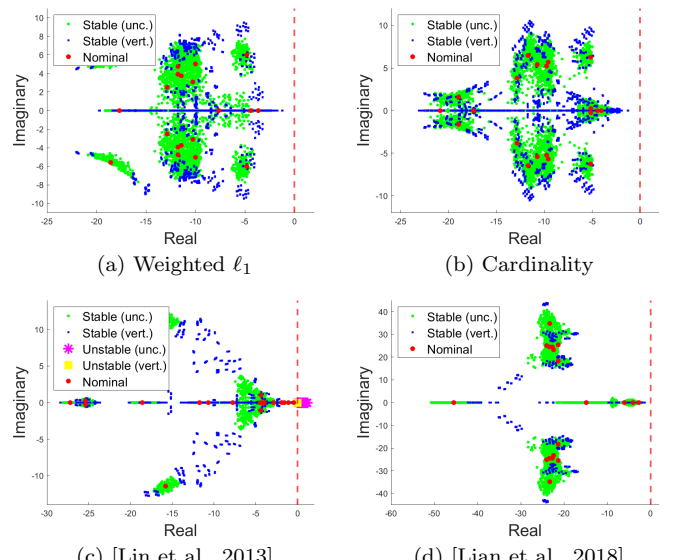


Fig. 3. Pole locations for $\sum_{i,j} \text{card}(\|\mathbf{K}_{ij}\|_F) = 24$; “(unc.)” denotes poles from randomly generated uncertain dynamics of each agent, “(vert.)” denote poles from 256 vertices of polytopic uncertainty. The red dashed line indicates the boundary of the stable region.

dynamics. The same procedure as in [Lian et al., 2018, Chap. 5] is used to compute the uncertainty input and output channels, with the \mathcal{H}_∞ constraint parameter γ set to 1.25. After obtaining the controllers, stability is evaluated over 200 randomly generated true dynamics of each agent, as well as over 256 vertex combinations constructed from the 16 vertex matrices associated with the stable and unstable agents. In the latter case, the stability analysis is performed under the simplifying assumption that all stable agents follow the same vertex matrix from the polytope corresponding to stable agents, and all unstable agents follow the same vertex matrix from the polyhedron corresponding to unstable agents.

The results in Figure 2, 3 and 4 show the LQ performance, stability, and sparse structure of the network controllers resulting from the proposed method and reference approaches in [Lin et al., 2013; Lian et al., 2018]. In all cases, the sparsity-promotion method converges to a sparse controller structure. The approach in [Lin et al., 2013] achieves the best LQ performance but can lead to instability due

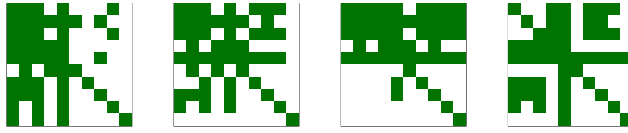


Fig. 4. Block structure of \mathbf{K} when $\sum_{i,j} \text{card}(\|\mathbf{K}_{ij}\|_F) = 50$; Green blocks denote nonzero blocks of \mathbf{K} . From left to right, the subfigures correspond to the results of the proposed algorithm with the weighted- ℓ_1 norm and cardinality, [Lin et al., 2013], and [Lian et al., 2018].

Table 1. Computation time when $N = 50$

Weighted ℓ_1	Cardinality [Lin et al., 2013]	[Lian et al., 2018]
8469 s	17276 s	4429 s

to the uncertain nature of each agent. Both versions of the proposed method, as well as the approach in [Lian et al., 2018], maintain stability under uncertain dynamics and for all vertex combinations of the polytopic uncertainty, with the proposed methods exhibiting superior LQ performance.

In practical scenarios such as wire-based communication, enforcing a symmetric controller structure is beneficial for reducing infrastructure requirements. Moreover, the system matrix \mathbf{A} in this example has a symmetric network with spatially decaying property, suggesting that a symmetric feedback controller is likely to be advantageous [Motee and Jadbabaie, 2008]. As shown in Figure 4, the proposed method with the cardinality penalty yields a symmetric sparse structure. These results demonstrate that the proposed methods achieve favorable LQ performance while preserving stability under system uncertainties using dissipativity, and can offer additional advantages in constructing practical communication architectures.

The total computation time is also evaluated for a larger network with $N = 50$ as in Table 1. In this case, \mathcal{H}_∞ constraint parameter γ is set to 8. Among the stabilizable algorithms, the proposed method with weighted ℓ_1 norm yields the shortest computation time, as it does not require any iterative procedure to determine a sparse communication topology.

6 Conclusion

This paper addressed the problem of dissipativity-based controller synthesis for networks of heterogeneous nonlinear agents, with the goal of identifying an appropriate communication structure. Since the original problem is NP hard, a combination of ADMM and ICO was employed to obtain a solution in a computationally tractable time. The applicability of the proposed strategy was demonstrated through a numerical example involving a network of both stable and unstable agents exhibiting uncertain dynamical behavior. The simulation results show that the proposed algorithms can identify network controllers with sparse and practically meaningful communication topologies while achieving moderate LQ performance and ensuring closed-loop stability under uncertainty. The current work focuses on full-state feedback controllers. However, the proposed strategy can be extended to dynamic output-feedback settings, which will be addressed in future work.

References

Babazadeh, M. and Nobakhti, A. (2016). Sparsity promotion in state feedback controller design. *IEEE Tr. Aut. Ctrl.*, 62(8), 4066–4072.

Boyd, S., Parikh, N., Chu, E., Peleato, B., Eckstein, J., et al. (2011). Distributed optimization and statistical learning via the alternating direction method of multipliers. *F. T. Mach.*, 3(1), 1–122.

Bridgeman, L.J. and Forbes, J.R. (2016). Conic bounds for systems subject to delays. *IEEE Tr. Aut. Ctrl.*, 62(4), 2006–2013.

Fardad, M., Lin, F., and Jovanović, M.R. (2011). Sparsity-promoting optimal control for a class of distributed systems. In *Proc. Amer. Ctrl. Conf.*, 2050–2055. IEEE.

Gupta, S. (1996). Robust stabilization of uncertain systems based on energy dissipation concepts. Technical report, NASA.

Hill, D. and Moylan, P. (2003). The stability of nonlinear dissipative systems. *IEEE Tr. Aut. Ctrl.*, 21(5), 708–711.

Jovanović, M.R. and Dhangra, N.K. (2016). Controller architectures: Tradeoffs between performance and structure. *Eu. J. Ctrl.*, 30, 76–91.

Khalil, I., Doyle, J., and Glover, K. (1996). *Robust and optimal control*, volume 2. Prentice hall New York.

Lian, F., Chakrabortty, A., and Duel-Hallen, A. (2017). Game-theoretic multi-agent control and network cost allocation under communication constraints. *IEEE journal on selected areas in communications*, 35(2), 330–340.

Lian, F., Chakrabortty, A., Wu, F., and Duel-Hallen, A. (2018). Sparsity-constrained mixed H_2/H_∞ control. In *Proc. Amer. Ctrl. Conf.*, 6253–6258. IEEE.

Lin, F., Fardad, M., and Jovanović, M.R. (2013). Design of optimal sparse feedback gains via the alternating direction method of multipliers. *IEEE Tr. Aut. Ctrl.*, 58(9), 2426–2431.

LoCicero, E.J. and Bridgeman, L. (2022). Sparsity promoting fixed-order H_2 -conic control. In *Proc. Amer. Ctrl. Conf.*, 4862–4867. IEEE.

LoCicero, E.J. and Bridgeman, L. (2025). Dissipativity-augmented multiobjective control of networks. *International Journal of Control*, 1–16.

Lozano, R., Brogliato, B., Egeland, O., and Maschke, B. (2013). *Dissipative systems analysis and control: theory and applications*. Springer Science & Business Media.

Motee, N. and Jadbabaie, A. (2008). Optimal control of spatially distributed systems. *IEEE Tr. Aut. Ctrl.*, 53(7), 1616–1629.

Moylan, P. and Hill, D. (2003). Stability criteria for large-scale systems. *IEEE Tr. Aut. Ctrl.*, 23(2), 143–149.

Natarajan, B.K. (1995). Sparse approximate solutions to linear systems. *SIAM journal on computing*, 24(2), 227–234.

Negi, N. and Chakrabortty, A. (2020). Sparsity-promoting optimal control of cyber-physical systems over shared communication networks. *Automatica*, 122, 109217.

Ren, Y., Li, Q., Liu, K.Z., and Ding, D.W. (2021). A successive convex optimization method for bilinear matrix inequality problems and its application to static output-feedback control. *I. J. Robu. Nonl. Ctrl.*, 31(18), 9709–9730.

Romer, A., Montenbruck, J.M., and Allgöwer, F. (2017). Determining dissipation inequalities from input-output samples. *IFAC-PapersOnLine*, 50(1), 7789–7794.

Sebe, N. (2018). Sequential convex overbounding approximation method for bilinear matrix inequality problems. *IFAC-PapersOnLine*, 51(25), 102–109.

Vidyasagar, M. (1981). *Input-output analysis of large-scale interconnected systems: decomposition, well-posedness and stability*. Springer.

Walsh, A. and Forbes, J.R. (2019). Interior-conic polytopic systems analysis and control. *ArXiv*.

Warner, E. and Scruggs, J. (2017). Iterative convex overbounding algorithms for bmi optimization problems. *IFAC-PapersOnLine*, 50(1), 10449–10455.

Willems, J.C. (1972). Dissipative dynamical systems part i: General theory. *Ar. rat. mech. analy.*, 45(5), 321–351.

Zakeri, H. and Antsaklis, P.J. (2022). Passivity measures in cyberphysical systems design: An overview of recent results and applications. *Ctrl. Sys. M.*, 42(2), 118–130.